Chapter 9
Pricing the Power of Wind

9.1 Introduction

In this book, the various aspects of weather derivative have been presented. So far, we have focused on modeling and pricing temperature derivatives. In this chapter, we focus on wind derivatives. A model for the dynamics of the wind-generating process using a nonparametric nonlinear wavelet network is presented. Moreover, the proposed methodology is compared against alternative methods, proposed in prior studies, and the pricing equations for wind futures are provided.

The notional value of the traded wind-linked securities is around $36 million indicating a large and growing market (WRMA 2009). However, after the close of the US Future Exchange, wind derivatives are traded in the Chicago Climate Futures Exchange and in the OTC. The demand from these derivatives exists. However, investors hesitate to enter into wind contracts. The main reasons of the slow growth of the wind market compared to temperature contracts are the difficulty in accurately modeling wind and the challenge to find a reliable model for valuing related contracts. As a result, there is a lack of reliable valuation framework that makes financial institutions reluctant to quote prices over these derivatives.

The aim of this chapter is to model and price wind derivatives. Wind derivatives are standardized products that depend only on the daily average wind speed measured by a predefined meteorological station over a specified period and can be used by wind (and weather in general)-sensitive business such as wind farms, transportation companies, construction companies, and theme parks to name a few. The financial contracts that are traded are based on the simple daily average wind speed index, and this is the reason that we choose to model only the dynamics of the daily average wind speeds. The revenues of each company have a unique dependence and sensitivity to wind speeds. Although wind derivatives and weather derivatives can hedge a significant part of the weather risk of the company always, some basis risk will still exist which must be hedged from each company separately. This can be done either by defining a more complex wind index or by taking an additional hedging position.

A.K. Alexandridis and A.D. Zapranis, *Weather Derivatives: Modeling and Pricing Weather-Related Risk*, DOI 10.1007/978-1-4614-6071-8_9,

Wind is free, renewable, and environmentally friendly source of energy (Billinton et al. 1996). While the demand for electricity is closely related to the temperature, the electricity produced by a wind farm is dependent on the wind conditions. The risk exposure of the wind farm depends on the wind speed and the wind direction and in some cases on the wind duration of the wind speed at certain level. However, modern wind turbines include mechanisms that allow turbines to rotate on in the appropriate wind direction (Caporin and Pres 2010). However, the underlying wind indices do not account for the duration of the wind speed at certain level but rather, usually, measure the average daily wind speed. Hence, the parameter of the duration of the wind speed at certain level is not considered in our daily model. Hence, the risk exposure of a wind farm can be analyzed by quantifying only the wind speed. On the other hand, companies like wind farms that its revenues depend on the duration effect can use an additional hedging strategy that includes this parameter. This can be done by introducing a second index that measures the duration. A similar index for temperature is the frost day index.

Many different approaches have been proposed so far for modeling the dynamics of the wind speed process. The most common is the generalized ARMA approach. There have been a number of studies on the use of linear ARMA models to simulate and forecast wind speed in various locations (Saltyte-Benth and Benth 2010; Billinton et al. 1996; Caporin and Pres 2010; Castino et al. 1998; Daniel and Chen 1991; Huang and Chalabi 1995; Kamal and Jafri 1997; Martin et al. 1999; Tol 1997; Torres et al. 2005). In Kavasseri and Seetharaman (2009), a more sophisticated ARFIMA model was used. Most of these studies did not consider in detail the accuracy of the wind speed forecasts (Huang and Chalabi 1995). On the other hand, Ailliot et al. (2006) apply an AR with time-varying coefficients to describe the space–time evolution of wind fields. In Benth and Saltyte-Benth (2009), a stochastic process called CAR model is introduced in order to model and forecast daily wind speeds. Finally, in Nielsen et al. (2006), various statistical methods were presented for short-term wind speed forecasting. Sfetsos (2002) argues about the use of linear or meteorological models since their prediction error is not significantly lower than the elementary persistent method. Alternatively, some studies use space–state models to simultaneously fit the speed and the direction of the wind (Castino et al. 1998; Cripps et al. 2005; Haslett and Raftery 1989; Martin et al. 1999; Tolman and Booij 1998; Tuller and Brett 1984).

Alternatively to the linear models, artificial intelligence was applied in wind speed modeling and forecasting. In Alexiadis et al. (1998), Barbounis et al. (2006), Beyer et al. (1994), More and Deo (2003), Sfetsos (2000), Mohandes et al. (1998), and Sfetsos (2002), neural networks were applied in order to model the dynamics of the wind speed process. In Mohandes et al. (2004), support vector machines were used while in Pinson and Kariniotakis (2003), and fuzzy neural networks were applied.

Depending on the application, wind modeling is based on hourly (Ailliot et al. 2006; Castino et al. 1998; Daniel and Chen 1991; Kamal and Jafri 1997; Martin et al. 1999; Sfetsos 2000, 2002; Torres et al. 2005; Yamada 2008), daily (Benth and Saltyte-Benth 2009; Billinton et al. 1996; Caporin and Pres 2010; Huang and Chalabi 1995; More and Deo 2003; Tol 1997), weekly, or monthly basis (More

and Deo 2003). When the objective is to hedge against electricity demand and production, hourly modeling is used, while for weather derivative pricing, the daily method is used. More rarely, weekly or monthly modeling is used in order to estimate monthly wind indexes. Since we want to focus on weather derivative pricing, the daily modeling approach is followed; however, the proposed method can be easily adapted in hourly modeling too.

Wind speed modeling is much more complicated than temperature modeling since wind has a direction and is greatly affected by the surrounding terrain such as building and trees (Jewson et al. 2005). However, in Benth and Saltyte-Benth (2009), it is shown that wind speed dynamics share a lot of common characteristics with the dynamics of temperature derivatives as it was found on Benth and Saltyte-Benth (2007), Zapranis and Alexandridis (2008, 2009, 2011), and Alexandridis (2010). In this context, we use a mean-reverting Ornstein–Uhlenbeck stochastic process to model the dynamics of the wind speed dynamics where the innovations are driven by a Brownian motion. The statistical analysis reveals seasonality in the mean and variance. In addition, we use a novel approach to model the autocorrelation of the wind speeds. More precisely, a WN is applied in order to capture accurately the autoregressive characteristics of the wind speeds.

The evaluation of the proposed methodology against alternative modeling procedures proposed in prior studies indicates that WNs can accurately model and forecast the dynamics and the evolution of the speed of the wind. The performance of each method was evaluated in-sample as well as out-of-sample and for different time periods.

The rest of the chapter is organized as follows: in Sect. 9.2, a statistical analysis of the wind speed dynamics is presented. In Sects. 9.2.1 and 9.2.2, a linear ARMA model and a nonlinear nonparametric WN is applied, respectively. The evaluation of the studied models is presented in Sect. 9.2.3. In Sect. 9.3, we derive the pricing formulas for future derivatives written on the wind index. Finally, in Sect. 9.4, we conclude.

9.2 Modeling the Daily Average Wind Speed

In this section, we derive empirically the characteristics of the daily average wind speed (DAWS) dynamics in New York, USA. The data were collected from NOAA[1] and correspond to DAWSs. The wind speed is measured in 0.1 knots. The measurement period is between 1st January 1988 and 28th February 2008. The first 20 years are used for the estimation of the parameters, while the remaining 2 months are used for the evaluation of the performance of the proposed model. In order for each year to have the same number of observations, the 29th of February

[1] http://www.noaa.gov

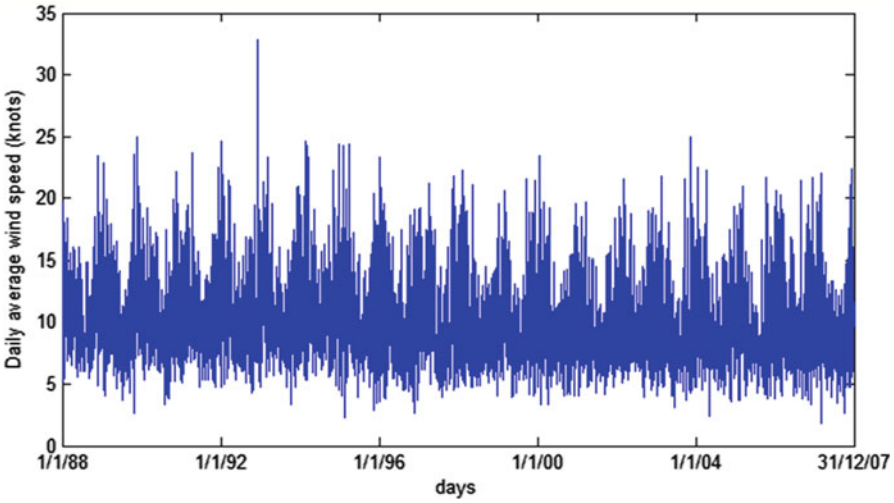

Fig. 9.1 Daily average wind speed for New York

Table 9.1 Descriptive statistics of the wind in New York

	Mean	Median	Max	Min	St. dev.	Skew	Kurt	J–B	*p* value
Original	9.91	9.3	32.8	1.8	3.38	0.96	4.24	1595.41	0
Transformed	2.28	2.3	3.6	0.6	0.34	0.00	3.04	0.51	1

J–B Jarque–Bera statistic, *P value p* values of the J–B statistic

is removed from the data resulting to 7,359 data points. The time series is complete without any missing values.

In Fig. 9.1, the DAWSs for the first 20 years are presented. A closer inspection of Fig. 9.1 reveals seasonality. The descriptive statistics of the in-sample data are presented in Table 9.1. The values of the data are always positive and range from 1.8 to 32.8 with mean around 9.91. The descriptive statistics of the DAWSs indicate that there is a strong positive kurtosis and skewness, while the normal hypothesis is rejected based on the Jarque–Bera statistic. The same conclusion can be reached observing the first part of Fig. 9.2 where the histogram of the DAWSs is represented. It is clear that the density of the DAWSs has positive skewness and excess kurtosis. Hence, the distribution of DAWSs deviates significantly from the normal, and it is not symmetrical. In literature, the Weibull or Rayleigh (which is a special case of the Weibull) distributions were proposed (Benth and Saltyte-Benth 2009; Saltyte-Benth and Benth 2010; Brown et al. 1984; Celik 2004; Daniel and Chen 1991; Garcia et al. 1998; Justus et al. 1978; Kavak Akpinar and Akpinar 2005; Nfaoui et al. 1996; Torres et al. 2005; Tuller and Brett 1984). In addition, some studies propose the use of the lognormal distribution (Benth and Saltyte-Benth 2009; Garcia et al. 1998) or the Chi-square (Dorvlo 2002). Finally, in Jaramillo and Borja (2004), a bimodal Weibull and Weibull distribution are used. However, empirical studies favor the use of the Weibull distribution (Celik 2004; Tuller and Brett 1984).

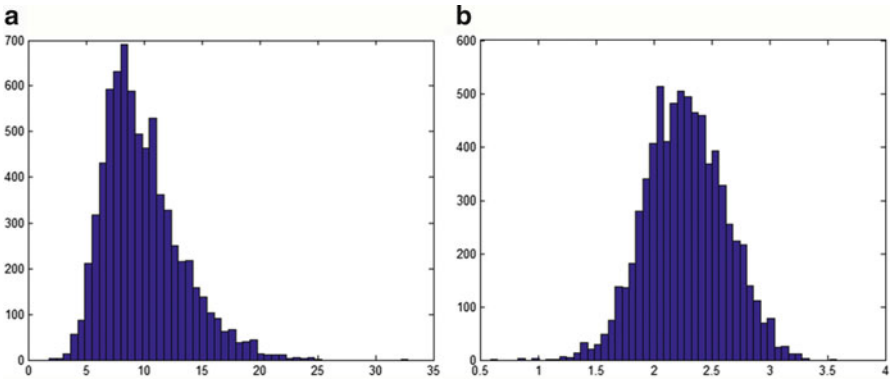

Fig. 9.2 Histogram of the (**a**) original and (**b**) Box–Cox transformed data

A closer inspection of part (a) of Fig. 9.2 reveals that the DAWSs in New York follow a Weibull distribution with scale parameter $\lambda = 11.07$ and shape parameter $k = 3.04$. Following Benth and Saltyte-Benth (2009), Brown et al. (1984), Daniel and Chen (1991), in order to symmetrize the data, the Box–Cox transform is applied. The Box–Cox transformation is given by

$$W^{(l)} = \begin{cases} \dfrac{W^l - 1}{l} & l \neq 0 \\ \ln(W) & l = 0 \end{cases} \tag{9.1}$$

where $W^{(l)}$ is the transformed data. The parameter l is estimated by maximizing the log-likelihood function. Note that the log transform is a special case of the Box–Cox transform with $l = 0$. The optimal l of the Box–Cox transform for the DAWSs in New York is estimated to be 0.014. In the second part of Fig. 9.2, the histogram of the transformed data can be found, while the second row on Table 9.1 shows the descriptive statistics of the transformed data.

The DAWSs exhibit a clear seasonal pattern which is preserved in the transformed data. The same conclusion can be reached by examining the ACF of the DAWS in the first part of Fig. 9.3. In Benth and Saltyte-Benth (2009), Saltyte-Benth and Benth (2010), and Caporin and Pres (2010), the seasonality was captured by series of sinusoids. As in Zapranis and Alexandridis (2008, 2009, 2011) and as it was presented in the previous chapters for the case of temperature process, the seasonal effects are modeled by a truncated Fourier series given by

$$S(t) = a_0 + b_0 t + \sum_{i=1}^{I_1} a_i \sin(2\pi i(t - f_i)/365) + \sum_{j=1}^{J_1} b_j \sin\big(2\pi j\big(t - g_j\big)/365\big). \tag{9.2}$$

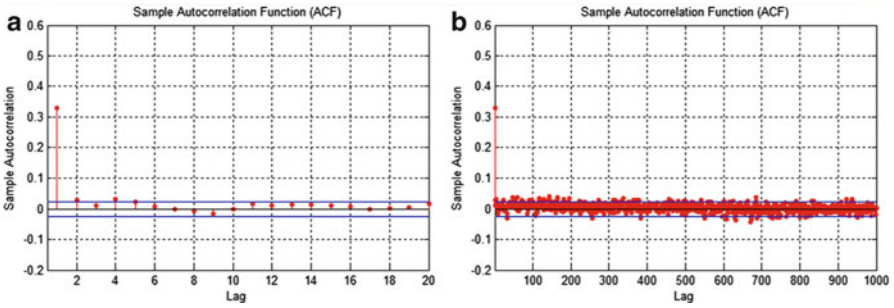

Fig. 9.3 The autocorrelation function of the transformed DAWSs in New York (**a**) before and (**b**) after removing the seasonal mean

Table 9.2 Estimated parameters of the seasonal component

a_0	b_0	a_1	f_1	b_1	g_1
2.3632	−0.000024	0.0144	827.81	0.1537	28.9350

In addition, we examine the data for a linear trend representing the global warming or the urbanization around the meteorological station. First, we quantify the trend by fitting a linear regression to the DAWS data. The regression is statistically significant with intercept $a_0 = 2.3632$ and $b_0 = -0.000024$ indicating a slight decrease in the DAWSs. Next, the seasonal periodicities are removed from the detrended data. The remaining statistically significant parameters of (9.2) with $I_1 = J_1 = 1$ are presented in Table 9.2. As it is shown on the second part of Fig. 9.3, the seasonal mean was successfully removed. The same conclusion was reached in previous studies for daily models for both temperature and wind (Alexandridis 2010; Zapranis and Alexandridis 2008, 2009, 2011; Benth et al. 2009; Benth and Saltyte-Benth 2005, 2007, 2009; Benth et al. 2007).

9.2.1 The Linear ARMA Model

In literature, various methods for studying the statistical characteristics of the wind speed, in daily or hourly measurements, were proposed. However, the majority of the studies utilize variations of the general ARMA model (Ailliot et al. 2006; Billinton et al. 1996; Brett and Tuller 1991; Daniel and Chen 1991; Huang and Chalabi 1995; Kamal and Jafri 1997; Lei et al. 2009; Nfaoui et al. 1996; Rehman and Halawani 1994; Torres et al. 2005). In this chapter, we will first estimate the dynamics of the detrended and deseasonalized DAWSs process using a general ARMA model, and then we will compare our results with a WN.

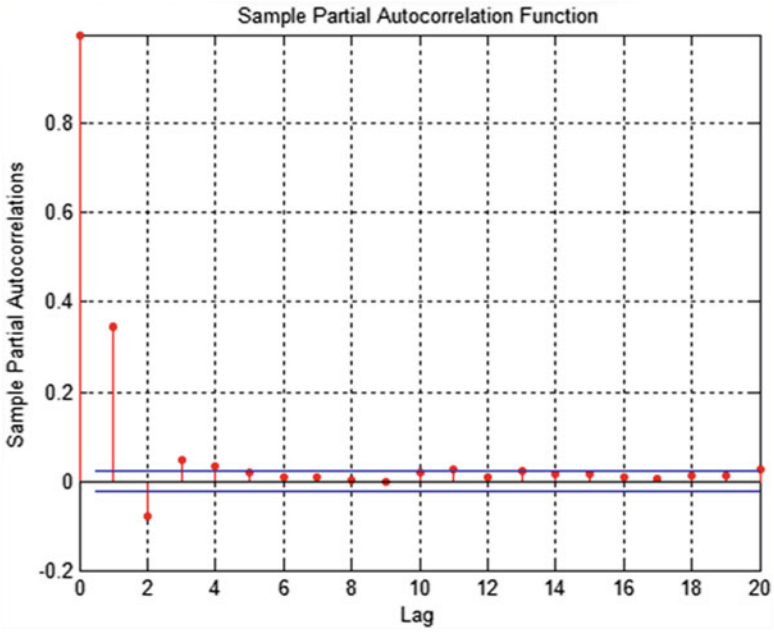

Fig. 9.4 The partial autocorrelation function of the detrended and deseasonalized DAWS in New York

We define the detrended and deseasonalized DAWS as

$$\tilde{W}^{(l)}(t) = W^{(l)}(t) - S(t). \tag{9.3}$$

The dynamics of $\tilde{W}^{(l)}(t)$ are modeled by an O–U stochastic process:

$$d\tilde{W}^{(l)}(t) = \kappa \tilde{W}^{(l)}(t)dt + \sigma(t)dB_t. \tag{9.4}$$

First, in order to select the correct ARMA model, we examine the ACF of the detrended and deseasonalized DAWS. A closer inspection of the second part of Fig. 9.3 reveals that the 1st, 2nd, and the 4th lags are significant. On the other hand, by examining the PACF in Fig. 9.4, we conclude that the first four lags are necessary to model the autoregressive effects of the wind speed dynamics.

In order to find the correct model, we estimate the log-likelihood function (LLF) and the Akaike information criterion (AIC). Consistent with the PACF, both criteria suggest that an AR (4) model is adequate for modeling the wind process since they were minimized when a model with four lags was used. The estimated parameters and the corresponding p values are presented in Table 9.3. It is clear that the three first parameters are statistically very significant since their p value is less than 0.05.

Table 9.3 Estimated parameters of the linear AR (4) model

Parameter	AR (1)	AR (2)	AR (3)	AR (4)
Value	0.3617	−0.0999	0.0274	0.0216
P value	0.0000	0.0000	0.0279	0.0657

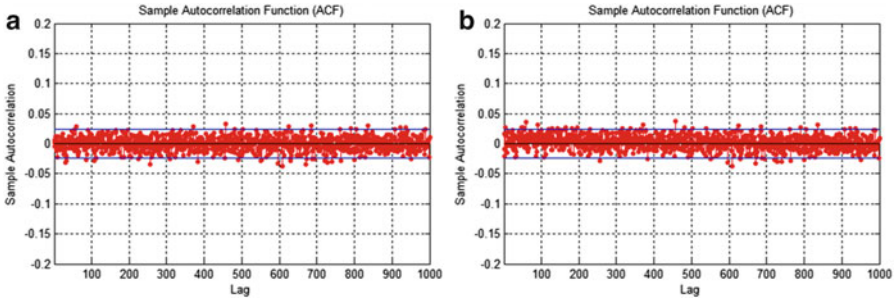

Fig. 9.5 Autocorrelation function of the residuals of (**a**) the linear model and (**b**) the WN

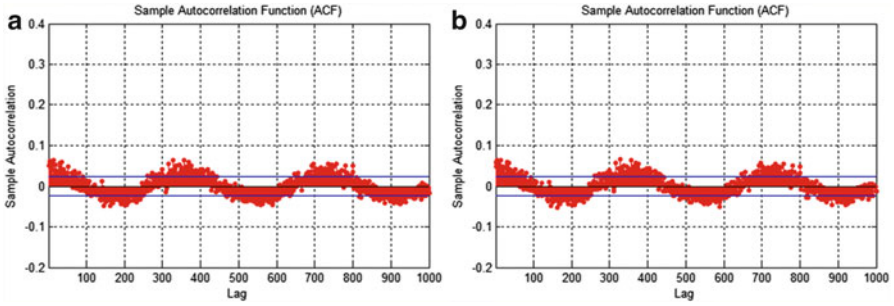

Fig. 9.6 Autocorrelation function of the squared residuals of (**a**) the linear model and (**b**) the WN

The parameter of the 4th lag is statistically significant with p value 0.0657. The AIC for this model is 0.46852, while the LLF is −1,705.14.

Observing the residuals of the AR model in the first part of Fig. 9.5, we conclude that the autocorrelation was successfully removed. However, the ACF of the squared residuals indicates a strong seasonal effect in the variance of the wind speed as it is shown in Fig. 9.6. The same conclusion was reached in previous studies for daily models for both temperature and wind (Alexandridis 2010; Benth et al. 2009; Benth and Saltyte-Benth 2005, 2007, 2009; Benth et al. 2007; Zapranis and Alexandridis 2008, 2009, 2011). Following the similar procedure that was described in the previous chapters for the temperature, we model the seasonal variance with a truncated Fourier series:

$$\sigma^2(t) = c_0 + \sum_{i=1}^{I_2} c_i \sin(2\pi it/365) + \sum_{j=1}^{J_2} d_j \sin(2\pi jt/365). \tag{9.5}$$

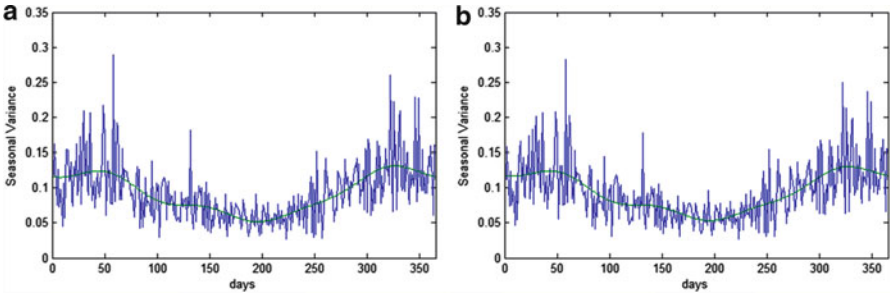

Fig. 9.7 Empirical and fitted seasonal variance of (**a**) the linear model and (**b**) the WN

Table 9.4 Estimated parameters of the seasonal variance in the case of the linear model

c_0	c_1	c_2	c_3	c_4	d_1	d_2	d_3	d_4
0.0932	0.000032	−0.0041	0.0015	−0.0028	0.0358	−0.0025	−0.0048	−0.0054

Table 9.5 Descriptive statistics of the residuals for the linear AR (4) model

Var	Mean	St. dev.	Max	Min	Skew	Kur	JB	*P* value	KS	*P* value	LBQ	P value
Noise	0	1	3.32	−5.03	−0.09	3.03	10.097	0.007	1.033	0.2349	8.383	0.989

St. dev. standard deviation, *JB* Jarque–Bera statistic, *KS* Kolmogorov–Smirnov statistic, *LBQ* Ljung–Box Q-statistic

Note that we assume that the seasonal variance is periodic and repeated every year, that is, $\sigma^2(t+365) = \sigma^2(t)$ where $t = 1, \ldots, 7359$. The empirical and the fitted seasonal variances are presented in Fig. 9.7, while in Table 9.4, the estimated parameters of (9.5) are presented. Non-surprisingly, the variance exhibits the same characteristics as in the case of temperature (Alexandridis 2010; Zapranis and Alexandridis 2008; Benth and Saltyte-Benth 2007). More precisely, the seasonal variance is higher in the winter and early summer, while it reaches its lower values during the summer period.

Finally, the descriptive statistics of the final residuals are examined. A closer inspection of Table 9.5 shows that the autocorrelation has successfully removed as indicated by the Ljung–Box Q-statistic. In addition, the distribution of the residuals is very close to the normal distribution as it is shown on the first part of Fig. 9.8; however, small negative skewness exists. More precisely, the residuals have mean 0 and standard deviation of 1. In addition, the kurtosis is 3.03 and the skewness is −0.09.

9.2.2 *Wavelet Networks for Wind Speed Modeling*

In this section, WNs are used in the transformed, detrended, and deseasonalized wind speed data in order to model the daily dynamics of wind speeds in New York.

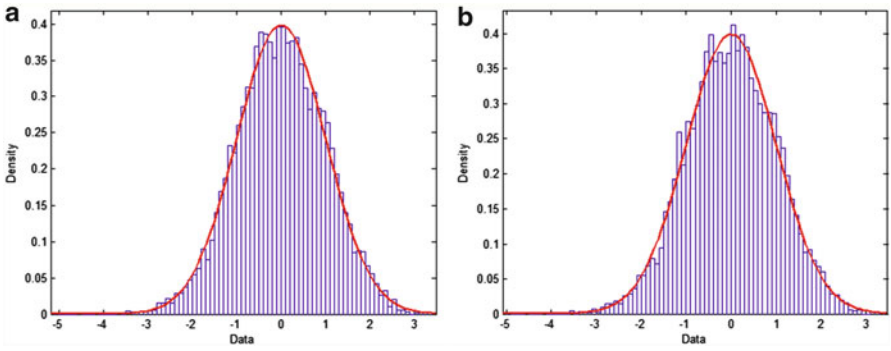

Fig. 9.8 Empirical and fitted normal distribution of the final residuals of the WN

Motivated by the waveform of the data, we expect a wavelet function to better fit the wind speed. In addition, it is expected that the nonlinear form of the WN will provide more accurate representation of the dynamics of the wind speed process both in-sample and out-of-sample.

The structure and the mathematical expressions of a WN are presented analytically in Appendices A and B, while in Alexandridis (2010), detailed explanation of how to use WNs in model identification problems is described. Since WNs are nonlinear tools, criteria like AIC or LLF cannot be used. Hence, in this section, WNs will be used in order to select the significant lags, to select the appropriate network structure, to train a WN in order to learn the dynamics of the wind speeds, and finally, to forecast the future evolution of the wind speeds.

The algorithm developed by Alexandridis (2010) simultaneously estimates the correct number of lags that must be used in order to model the wind speed dynamics and the architecture of the WN by using a recurrent algorithm. An illustration of the model identification algorithm is presented in Appendix A.

Our backward elimination algorithm examines the contribution of each available explanatory variable to the predictive power of the WN. First, the prediction risk of the WN is estimated as well as the statistical significance of each variable. If a variable is statistically insignificant, it is removed from the training set, and the prediction risk and the new statistical measures are estimated. The algorithm stops if all explanatory variables are significant. Hence, in each step of our algorithm, the variable with the larger p value greater than 0.1 will be removed from the training set of our model. After each variable removal, a new architecture of the WN will be selected and a new WN will be trained. However, the correctness of the decision of removing a variable must be examined. This can be done either by examining the prediction risk or the $\bar{R}^2$. If the new prediction risk is smaller than the new prediction risk multiplied by a threshold, then the decision of removing the variable was correct. If the prediction risk increased more than the allowed threshold, then the variable was reintroduced back to the model. We set this threshold at 5%. In this study, the selected statistical measure is the SBP proposed by Moody and Utans (1992). Previous analysis in Alexandridis (2010) indicates that the SBP fitness

Table 9.6 Variable selection with backward elimination in New York

Step	Variable to remove (lag)	Variable to enter (lag)	Variables in model	Hidden units (parameters)	*N*/*P* ratio	Empirical loss	Prediction risk
–			7	1 (23)	317.4	0.0467	0.0938
1	7	–	6	1 (20)	365.0	0.0467	0.0940
2	5	–	5	1 (17)	429.4	0.0467	0.0932
3	6	–	4	2 (23)	317.4	0.0467	0.0938
4	4	-	3	2 (18)	405.6	0.0468	0.0937

The algorithm concluded in four steps. In each step, the following are presented: which variable is removed, the number of hidden units for the particular set of input variables and the parameters used in the wavelet network, the ratio between the parameters and the training patterns, the empirical loss, and the prediction risk

criterion was found to significantly outperform alternative criteria in the variable selection algorithm. The SBP quantifies the effect on the empirical loss of replacing a variable by its mean. Analytical description of the SBP is given in Alexandridis (2010), Zapranis and Refenes (1999), and Moody and Utans (1992). In each step, the SBP and the corresponding p value are calculated. For analytical explanation of each step of the algorithm, we refer to Alexandridis (2010).

The proposed variable selection framework will be applied on the transformed, detrended, and deseasonalized wind speeds in New York in order to select the length of the lag series. The target values of the WN are the DAWSs. The explanatory variables are lagged versions of the target variable. The relevance of a variable to the model is quantified by the SBP criterion which was introduced in Moody and Utans (1992). Initially, the training set contains the dependent variable and seven lags. The analysis in the previous section indicates that a training set with seven lags will provide all the necessary information of the ACF of the detrended and deseasonalized DAWSs. Hence, the training set consists of 7 inputs, 1 output, and 7,293 training pairs.

Table 9.6 summarizes the results of the model identification algorithm for New York. Both the model selection and the variable selection algorithms are included in Table 9.6. The algorithm concluded in four steps and the final model contains only three variables, that is, three lags. The prediction risk for the reduced model is 0.0937 while for the original model was 0.0938. On the other hand, the empirical loss slightly increased from 0.0467 for the initial model to 0.0468 for the reduced model indicating that the explained variability (unadjusted) slightly decreased. Finally, the complexity of the network structure and number of parameters were significantly reduced in the final model. The initial model needed one hidden unit (HU) and seven inputs. Hence, 23 parameters were adjusted during the training phase. Hence, the ratio of the number of training pairs n to the number of parameters p was 317.4. In the final model, only two HU and three inputs were used. Hence, only 18 parameters were adjusted during the training phase, and the ratio of the number of training pairs n to the number of parameters p was 405.6.

The proposed algorithm suggests that a WN needs only three lags to extract the autocorrelation from the data while the linear model needed four lags. A closer inspection of Table 9.6 reveals that the WN with three and four lags have the same

Table 9.7 Estimated parameters of the seasonal variance in the case of the WN

c_0	c_1	c_2	c_3	c_4	d_1	d_2	d_3	d_4
0.0935	−0.000020	−0.0034	0.0014	−0.0026	0.0353	−0.0016	−.0042	−0.0052

Table 9.8 Descriptive statistics of the residuals for the WN model

Var	Mean	St. dev	Max	Min	Skew	Kur.	JB	*P* value	KS	*P* value	LBQ	*P* value
noise	0	1	3.32	−4.91	−0.08	3.04	8.84	0.0043	0.927	0.3544	13.437	0.858

St. dev. standard deviation, *JB* Jarque–Bera statistic, *KS* Kolmogorov–Smirnov statistic, *LBQ* Ljung–Box Q-statistic

predictive power in-sample and out-of-sample. Hence, we chose the simpler model. Our model is similar to an AR (3) model with time-varying parameters.

Examining the second part of Fig. 9.5, we conclude that the autocorrelation was successfully removed from the data; however, the seasonal autocorrelation in the squared residuals is still present as it is shown in Fig. 9.6. We will remove the seasonal autocorrelation using (9.5). The estimated parameters are presented in Table 9.7, and as it was expected, their values are similar to those of the case of the linear model. In Fig. 9.7, the empirical and the fitted seasonal variance is presented. Again, the same conclusions are reached for the seasonal variance. The variance is higher at winter period, while it reaches its minimum during the summer period.

Finally, examining the final residuals of the WN model, we observe that the distribution of the residuals is very close to the normal distribution as it is shown in Fig. 9.8, while the autocorrelation was successfully removed from the data. In addition, we observe an improvement in the distributional statistics in contrast to the case of the linear model. The distributional statistics of the residuals are presented in Table 9.8.

Concluding, the distributional statistics of the residuals indicate that in in-sample, the two models can accurately represent the dynamics of the DAWSs; however, an improvement is evident when a nonlinear nonparametric WN is used.

9.2.3 Forecasting Daily Average Wind Speeds

In this section, our proposed model will be validated out-of-sample. In addition, the performance of our model will be tested against two models, first, against the linear model previously described and, second, against the simple persistent method usually referred as benchmark. The linear model is the AR (4) model described in the previous section. The persistent method assumes that today's and tomorrow's DAWSs will be equal, that is, $W^*(t+1) = W(t)$ where the W^* indicates the forecasted value.

Table 9.9 Out-of-sample comparison. One month

	Persistent	AR (4)	WN
Md.AE	2.3000	2.2147	2.1081
MAE	3.3000	2.5547	2.5026
Max AE	8.2000	7.9217	7.7590
SSE	507.9300	328.9947	320.2573
RMSE	4.0478	3.2577	3.2142
NMSE	1.5981	1.0351	1.0076
MSE	16.3848	10.6127	10.3309
MAPE	0.3456	0.2744	0.2680
SMAPE	0.3233	0.2570	0.2518
POCID	47%	80%	80%
IPOCID	33%	33%	37%
POS	100%	100%	100%

Md. AE median absolute error, *MAE* mean absolute error, *Max AE* maximum absolute error, *SSE* sum of squared errors, *RMSE* root-mean-square error, *NMSE* normalized mean square error, *MSE* mean square error, *MAPE* mean absolute percentage error, *SMAPE* symmetric MAPE, *POCID* position of change in direction, *IPOCID* independent POCID, *POS* position of sign

The three models will be used for forecasting DAWSs for two different periods. Usually, wind derivatives are written for a period of a month. Hence, DAWSs for 1 and 2 months will be forecasted. The out-of-sample dataset correspond to the period from January 1 to February 28, 2008, and were not used for the estimation of the linear and nonlinear models. Note that our previous analysis reveals that the variance is higher in the winter period indicating that it is more difficult to forecast accurately DAWS for these two months.

In Table 9.9, the performance of the three methods when the forecast window is 1 month is presented. Various error criteria are estimated like the mean, median, and max. AE; the mean square error (MSE); the POCID; and the IPOCID. As it is shown on Table 9.9, our proposed method outperforms both the persistent and the AR (4) model. The AR (4) model performs better than the naïve persistent method; however, all error criteria are improved when a nonlinear WN is used. The MSE is 16.3848 for the persistent method, 10.6127 for the AR (4) model, and 10.3309 for the WN. In addition, our model can predict more accurately the movement of the wind speed since the POCID is 80% for the WN and the AR (4) models, while it is only 47% for the persistent method. Moreover, the IPOCID is 37% for the proposed model, while it is only 33% for the other two methods.

In order to compare our model directly with the linear method, we estimate a linear AR (3) model. However, our proposed methodology still outperforms the linear method.

Next, the three forecasting methods are evaluated in 2 months day-ahead forecasts. The results are similar and presented in Table 9.10. The proposed WN outperforms the other two methods. Only the max. AE and the POCID are slightly smaller when the AR (4) model is used. However, the IPOCID is 38% for both methods. Also, our results indicate that the persistent method produces significantly

Table 9.10 Out-of-sample comparison. Two months

	Persistent	AR (4)	WN
Md.AE	2.4000	2.7981	2.6589
MAE	3.3678	2.8126	2.7976
Max AE	11.2000	7.9345	8.0194
SSE	1054.3500	706.1806	702.4437
RMSE	4.2273	3.4596	3.4505
NMSE	1.4110	0.9450	0.9400
MSE	17.8703	11.9692	11.9058
MAPE	0.3611	0.3014	0.3001
SMAPE	0.3289	0.2798	0.2782
POCID	45%	71%	69%
IPOCID	36%	38%	38%
POS	100%	100%	100%

Md. AE median absolute error, *MAE* mean absolute error, *Max AE* maximum absolute error, *SSE* sum of squared errors, *RMSE* root-mean-square error, *NMSE* normalized mean square error, *MSE* mean square error, *MAPE* mean absolute percentage error, *SMAPE* symmetric MAPE, *POCID* position of change in direction, *IPOCID* independent POCID, *POS* position of sign

Table 9.11 Estimation of the cumulative rainfall index for 1 and 2 months using an AR (4) model, WN, and historical burn analysis

	AR (4)	WN	HBA	Actual
1 month	305.1	312.7	345.5	311.2
2 months	579.5	591.1	658.3	600.6

worse forecasts. Finally, the WN and the linear AR (3) model are compared with first to show better forecasting ability.

Our results indicate that the WN can forecast the evolution of the dynamics of the DAWSs, and hence, they constitute an accurate tool for wind derivatives pricing.

In order to have a better insight of the performance of each method, the cumulative average wind speed (CAWS) index is calculated. Since we are interested in weather derivatives, one common index is the sum of the daily rainfall index over a specific period. In Table 9.11, the estimation of three methods is presented. More precisely, the WN, the AR (4), as well as the HBA methods are compared. The HBA is a simple statistical method that estimates the performance of the index over the specific period the previous years and it is often used in the industry. In other words, it is the average of 20 years of the index over the period of January and February, and it serves as a benchmark.

The final row of Table 9.11 presents the actual values of the cumulative rainfall index. An inspection of Table 9.11 reveals that the WN significantly outperforms the other two methods. For the first case, where forecasts for 1 month ahead are estimated, the forecast of the CAWS index using WN is 312.7, while the actual index is 311.2. On the other hand, the forecast using the AR (4) model is 305.1. However, when the forecast period increases, the forecast of the AR (4) model

significantly deviates. More precisely, for the second case, the forecast of the WN is 591.1 while the actual index is 600.6 and the AR (4) forecast is 579.5. Finally, we have to mention that the WN uses less information than the AR (4) model, since in the case of WN, only the information of three lags is used.

Since we are interested in wind derivatives and the valuation of wind contracts, next, an illustration of the performance of each method using a theoretical contract is presented. A common wind contract has a tick size of 0.1 knots and pays 20$ per tick size. Hence, for the case of a 1-month contract, the AR (4) method underestimates the contract size for 1,200$, while the WN overestimates the contract for 300$ only. Similarly, for the case of a 2-month contract, the AR (4) method underestimates the contract size for 4,220$, while the WN underestimates the contract for 1,900$.

Incorporating meteorological forecasts can lead to a potentially significant improvement of the performance of the proposed model. Meteorological forecasts can be easily incorporated in both the linear and the WN models previously presented. A similar approach was followed for temperature derivatives by Dorfleitner and Wimmer (2010) for temperature derivatives. However, this method cannot be always applied. Despite great advances in meteorological science, weather still cannot be predicted precisely and consistently, and forecasts beyond 10 days are not considered accurate (Wilks 2011). If the day that the contract is traded is during or close to the life of the derivative (during the period that wind measurements are considered), the meteorological forecasts can be incorporated in order to improve the performance of the methods. However, very often, weather derivatives are traded long before the start of the life of the derivative. More precisely, very often, weather derivatives are traded months or even a season before the starting day of the contract. In this case, meteorological forecasts cannot be used.

9.3 Pricing Wind Derivatives

In this section, the pricing formulas for wind derivatives are presented under the assumption of a normal driving noise process. The analysis performed in the previous section indicates that the assumption that the final residuals, after dividing out the seasonal variance, follow a normal distribution is justified.

When the market is complete, a unique risk-neutral probability measure $Q \sim P$ can be obtained, where P is the real-world probability measure. This change of measure turns the stochastic process into a martingale. Hence, financial derivatives can be priced under the risk-neutral measure by the discounted expectation of the derivative payoff.

The same implications that we faced in the pricing of temperature derivatives appear also in the pricing of wind derivatives. The wind market is an incomplete market. The underlying weather derivative cannot be stored or traded. Moreover, the market is relatively illiquid. In principle (extended), risk-neutral valuation can still be carried out in incomplete markets.

The method that was used in order to proceed in temperature derivative pricing will be followed also in this section. The change of measure from the real world to the risk-neutral world under the dynamics of a BM can be performed using the Girsanov's theorem.

The statistical analysis indicates that the transformed DAWSs can be modeled by a mean-reverting O–U process where the speed of mean reversion variable is a function of time:

$$dW_t^{(l)} = S(t) + a(t)\Big(W_{t-1}^{(l)} - S(t-1)\Big)dt + \sigma(t)dB_t, \tag{9.6}$$

where $S(t)$ is the seasonal function, $\sigma(t)$ is the seasonal variance which is bounded by zero, $a(t)$ is the speed of mean reversion, and B_t is the driving noise process.

Using the Girsanov's theorem, under the risk-neutral measure Q, we have that

$$dB_t^{\theta} = dB_t - \theta(t), \tag{9.7}$$

where $\theta(t)$ is the market price of risk and

$$\int_0^T \theta^2(t)dt < \infty. \tag{9.8}$$

Hence, applying Itô formula on (9.6) and (9.7), the solution of the transformed DAWS under the risk-neutral measure Q is given by

$$\begin{aligned} W_t^{(l)} = S(t) + e^{\int_0^t a(z)dz}\Big(W_0^{(l)} - S(0)\Big) + e^{\int_0^t a(z)dz}\int_0^t \sigma(s)\theta(s)e^{-\int_0^s a(z)dz}ds \\ + e^{\int_0^t a(z)dz}\int_0^t \sigma(s)e^{-\int_0^s a(z)dz}dB_t^{\theta}. \end{aligned} \tag{9.9}$$

The proposed model is an extension of the CAR (p) introduced by Brockwell and Marquardt (2005) and applied by Benth and Saltyte-Benth (2009) in wind derivative pricing. Hence, we follow a similar pricing approach presented in Benth and Saltyte-Benth (2009).

The transformed, detrended, and deseasonalized DAWS $\tilde{W}_t^{(l)} = W_t^{(l)} - S(t)$ are normally distributed with mean

$$\mu_{\theta}(t, s, \tilde{W}_t^{(l)}) = e^{\int_t^s a(z)dz}\tilde{W}_s^{(l)} + e^{\int_t^s a(z)dz}\int_t^s \sigma(u)\theta(u)e^{-\int_t^u a(z)dz}du, \tag{9.10}$$

and variance

$$\Sigma^2(t,s) = e^{2\int_t^s a(z)dz} \int_t^s \sigma^2(s) e^{-2\int_t^u a(z)dz} du. \tag{9.11}$$

The market price of wind risk is necessary in pricing wind derivatives. However, in order to estimate θ, the actual prices of derivatives are required. Since the shutdown of the US Future Exchange, wind derivatives are traded only in the Chicago Climate Futures Exchange and in the OTC market, and as a result, it is hard to obtain market data. Hence, it is very difficult to estimate the market price of wind risk. However, the trading volume of wind derivatives is increasing every year (WRMA 2010), and it is expected that wind derivatives will be soon included in the listed products of the CME.

A solution to this problem is presented by Benth et al. (2009) where they study the market price of risk for temperature derivatives in various Asian cities. The market price of risk was estimated by calibrating model prices. Their results indicate that the market price of risk for Asian temperature derivatives is different from zero and shows a seasonal structure that comes from the seasonal variance of the temperature process. Their empirical findings suggest that by knowing the formal dependence of the market price of risk on seasonal variation, one can infer the market price of risk for regions where weather derivative market does not exist.

Similarly, in Huang et al. (2008), a pricing method for temperature derivatives in Taiwan is presented. Since no active weather market exists in Taiwan, the parameter θ is approximated by a function of the market price of risk of the Taiwan Stock Exchange.

9.3.1 The Cumulative Average Wind Speed Index

In this section, we derive the pricing equation for the CAWS index. Similar to the CAT index, the CAWS index is the sum of the DAWSs over a specific period $[\tau_1, \tau_2]$, and it is given by

$$\text{CAWS} = \int_{\tau_1}^{\tau_2} W(s)ds. \tag{9.12}$$

Our aim is to give a mathematical expression for the CAWS future price. If Q is the risk-neutral probability and r is the constant compounding interest rate, then the arbitrage-free future price of a CAT contract at time $t \leq \tau_1 < \tau_2$ is given by

$$e^{-r(\tau_2 - t)} \mathrm{E}_Q \left[\int_{\tau_1}^{\tau_2} W(s)ds - F_{\text{CAWS}}(t, \tau_1, \tau_2) | \mathbf{F}_t \right] = 0, \tag{9.13}$$

and since F_{CAWS} is $\mathbf{F}_t$ adapted, we derive the price of a CAT futures to be

$$F_{\text{CAWS}}(t,\tau_1,\tau_2) = \mathrm{E}_Q\left[\int_{\tau_1}^{\tau_2} W(s)ds|\mathbf{F}_t\right]. \tag{9.14}$$

To derive the future price, we must calculate the conditional expectation of $W(s)$ given F_t, for $s \geq t$. This is done in the following Lemma, first presented in Benth and Saltyte-Benth (2009). For reasons of completeness, we reproduce this Lemma here.

Lemma 9.1 *Let $0 \leq t \leq s \leq T$, then for $l \in (0,1]$, it holds that*

$$E_Q[W(s)|\mathbf{F}_t] = M_{1/l}\left(1 + l\left(S(s) + \mu_\theta\left(t,s,\tilde{W}_t^{(l)}\right), l^2\Sigma^2(t,s)\right)\right), \tag{9.15}$$

where $M_k(a,b^2)$ is the k^{th} moment of a normal random variable with mean a and variance b^2 and $\mu_\theta\left(t,s,\tilde{W}_t^{(l)}\right)$ and $\Sigma^2(t,s)$ are given by (9.10) and (9.11), respectively.

Proof From (9.1) and (9.9), we have that the wind speed at time s given F_t can be represented (for $l \neq 0$) as

$$W(s) = \left[l\left(S(s) + \mu_\theta\left(t,s,\tilde{W}_t^{(l)}\right) + \Sigma(t,s)Z\right) + 1\right]^{\frac{1}{l}},$$

where Z is a standard normally distributed random variable independent of $\mathbf{F}_t$. Further, $\mu_\theta\left(t,s,\tilde{W}_t^{(l)}\right)$ is $\mathbf{F}_t$ measurable. Hence, the result follows from a direct calculation. The lognormal case $l = 0$ follows similarly.

□

Hence, the arbitrage-free price of the CAWS index easily follows from Lemma 9.1.

Proposition 9.1 *The arbitrage-free price of* CAWS *index at time $t \leq \tau_1 < \tau_2$ is given by*

$$F_{\text{CAWS}}(t,\tau_1,\tau_2) = \int_{\tau_1}^{\tau_2}\left(M_{1/l}\left(1 + l\left(S(s) + \mu_\theta\left(t,s,\tilde{W}_t^{(l)}\right), l^2\Sigma^2(t,s)\right)\right)\right)ds, \tag{9.16}$$

where $M_k(a,b^2)$ is the k^{th} moment of a normal random variable with mean a and variance b^2 and $\mu_\theta\left(t,s,\tilde{W}_t^{(l)}\right)$ and $\Sigma^2(t,s)$ are given by (9.10) and (9.11), respectively.

Proof We have from (9.14) that

$$F_{\text{CAWS}}(t,\tau_1,\tau_2) = \mathrm{E}_Q\left[\int_{\tau_1}^{\tau_2} W(s)ds|\mathbf{F}_t\right],$$

and using Itô's isometry, we can interchange the expectation and the integral

$$\mathrm{E}_Q\left[\int_{\tau_1}^{\tau_2} W(s)ds|\mathbf{F}_t\right] = \int_{\tau_1}^{\tau_2} \mathrm{E}_Q[W(s)|\mathbf{F}_t]ds,$$

and from a direct application from Lemma 9.1, we have that

$$F_{\text{CAWS}}(t,\tau_1,\tau_2) = \int_{\tau_1}^{\tau_2} M_{1/l}\Big(1 + l\Big(S(s) + \mu_\theta\Big(t,s,\tilde{W}_t^{(l)}\Big), l^2\Sigma^2(t,s)\Big)\Big)ds. \qquad \square$$

9.3.2 The Nordix Wind Speed Index

In this section, we derive the pricing equations for the Nordix wind speed index. The Nordix wind speed index is the index that the US Future Exchange used to settle wind derivatives. The Nordix index is given by

$$I(\tau_1,\tau_2) = 100 + \sum_{s=\tau_1}^{\tau_2}(W(s) - w_{20}(s)), \tag{9.17}$$

and measures the daily wind speed deviations from the mean of the past 20 years over a period $[\tau_1,\tau_2]$.

The result of Lemma 9.1 is applied again to derive the price of a Future Nordix wind speed index.

Proposition 9.2 *The arbitrage-free price of Nordix wind future speed index at time* $t \le \tau_1 < \tau_2$ *is given by*

$$\begin{aligned} F_{NWI}(t,\tau_1,\tau_2) = 100 &- \sum_{s=\tau_1}^{\tau_2} w_{20}(s) \\ &+ \sum_{s=\tau_1}^{\tau_2} M_{1/l}\Big(1 + l\Big(S(s) + \mu_\theta(t,s,\tilde{W}_t^{(l)}\Big), l^2\Sigma^2(t,s)\Big), \end{aligned} \tag{9.18}$$

where $M_k(a,b^2)$ *is the* k^{th} *moment of a normal random variable with mean a and variance* b^2.

Proof If Q is the risk-neutral probability and r is the constant compounding interest rate, then the arbitrage-free future price of a Nordix wind speed index contract at time $t \le \tau_1 < \tau_2$ is given by

$$e^{-r(\tau_2-t)}\mathrm{E}_Q\left[100-\sum_{s=\tau_1}^{\tau_2}w_{20}(s)+\sum_{s=\tau_1}^{\tau_2}W(s)-F_{NWI}(t,\tau_1,\tau_2)|\mathbf{F}_t\right]=0,$$

and since $F_{NWI}(t,\tau_1,\tau_2)$ is $\mathbf{F}_t$ adapted, we derive the price of a Nordix wind future index to be

$$F_{NWI}(t,\tau_1,\tau_2)=100-\sum_{s=\tau_1}^{\tau_2}w_{20}(s)+\mathrm{E}_Q\left[\sum_{s=\tau_1}^{\tau_2}W(s)|\mathbf{F}_t\right].$$

Applying the Lemma 4.1 from Benth and Saltyte-Benth (2009), we find the explicit solution for the price of the Nordix wind future index:

$$\begin{aligned}F_{NWI}(t,\tau_1,\tau_2)&=100-\sum_{s=\tau_1}^{\tau_2}w_{20}(s)\\&+\sum_{s=\tau_1}^{\tau_2}M_{1/l}\Big(1+l\Big(S(s)+\mu_\theta(t,s,\tilde{W}_t^{(l)})\Big),l^2\Sigma^2(t,s)\Big),\end{aligned}$$

where $M_k(a,b^2)$ is the k^{th} moment of a normal random variable with mean a and variance b^2.

□

9.4 Conclusions

In this chapter, DAWSs from New York were studied. Our analysis revealed strong seasonality in the mean and variance. The DAWSs were modeled by a mean-reverting Ornstein–Uhlenbeck process in the context of wind derivative pricing. In this study, the dynamics of the wind-generating process are modeled using a nonparametric nonlinear WN. Our proposed methodology was compared in-sample and out-of-sample against two methods often used in prior studies. The characteristics of the wind speed process are very similar to the process of daily average temperatures.

Our method is validated in a 2-month-ahead out-of-sample forecast period. Moreover, the various error criteria produced by the WN are compared against the linear AR model and the persistent method. Results show that the WN outperforms the other two methods, indicating that WNs constitute an accurate model for forecasting DAWSs. More precisely, the WN's forecasting ability is stronger in both samples. Testing the fitted residuals of the WN, we observe that the distribution of the residuals is very close to the normal. Also, the WN needed only the information of the past 3 days, while the linear method suggested a model with four lags. Finally, we provided the pricing equations for wind futures of the Nordix

index. Although we focused on DAWSs, our model can be easily adapted in hourly modeling.

The results in this chapter are preliminary and can be further analyzed. More precisely, alternative methods for estimating the seasonality in the mean and in the variance can be developed. Alternative methods could improve the fitting to the original data as well as the training of the WN.

Also, it is important to test the largest forecasting window of each method. Since meteorological forecasts of a window larger than few days are considered inaccurate, this analysis will suggest the best model according to the desired forecasting interval.

Finally, a large-scale comparison must be conducted. Testing the proposed methods as well as more sophisticated models, like general ARFIMA or GARCH, in various meteorological stations will provide a better insight in the dynamics of the DAWS as well as in the predictive ability of each method.

References

Ailliot P, Monbet V, Prevosto M (2006) An autoregressive model with time-varying coefficients for wind fields. Envirometrics 17:107–117

Alexandridis A (2010) Modelling and pricing temperature derivatives using wavelet networks and wavelet analysis. Ph.D. Thesis, University of Macedonia, Thessaloniki

Alexiadis MC, Dokopoulos PS, Sahsamanoglou HS, Manousaridis IM (1998) Short-term forecasting of wind speed and related electrical power. Solar Energy 63(1):61–68

Barbounis TG, Theocharis JB, Alexiadis MC, Dokopoulos PS (2006) Long-term wind speed and power forecasting using local recurrent neural network models. IEEE Trans Energy Convers 21 (1):273–284

Benth FE, Saltyte-Benth J (2005) Stochastic modelling of temperature variations with a view towards weather derivatives. Appl Math Finance 12(1):53–85

Benth FE, Saltyte-Benth J (2007) The volatility of temperature and pricing of weather derivatives. Quant Finance 7(5):553–561

Benth FE, Saltyte-Benth J (2009) Dynamic pricing of wind futures. Energy Econ 31:16–24

Benth FE, Saltyte-Benth J, Koekebakker S (2007) Putting a price on temperature. Scand J Stat 34:746–767

Benth FE, Hardle WK, Lopez Cabrera B (2009) Pricing of Asian temperature risk. SFB649 Working Paper. Humboldt-Universitat zu Berlin, Berlin

Beyer HG, Degner T, Hausmann J, Hoffmann M, Rujan P (1994) Short-term prediction of wind speed and power output of a wind turbine with neural networks. In: 2nd European congress on intelligent techniques and soft computing, Aachen, 20–23 Sept 1994

Billinton R, Chen H, Ghajar R (1996) Time-series models for reliability evaluation of power systems including wind energy. Microelectron Reliab 36(9):1253–1261

Brett AC, Tuller SE (1991) The autocorrelation of hourly wind speed observations. J Appl Meteorol 30(6):823–833. doi:10.1175/1520-0450(1991)030<0823:TAOHWS>2.0.CO;2

Brockwell PJ, Marquardt T (2005) Levy-driven and fractionality integrated ARMA process with continuous time parameter. Stat Sin 15:477–494

Brown BG, Katz RW, Murphy AH (1984) Time-series models to simulate and forecast wind speed and wind power. J Clim Appl Meteorol 23:1184–1195

Caporin M, Pres J (2010) Modelling and forecasting wind speed intensity for weather risk management. Comput Stat Data Anal. doi:doi:10.1016/j.csda.2010.06.019

Castino F, Festa R, Ratto CF (1998) Stochastic modelling of wind velocities time-series. J Wind Eng Ind Aerodyn 74–76:141–151
Celik AN (2004) A statistical analysis of wind power density based on the Weibull and Rayleigh models at the southern region of Turkey. Renew Energy 29(4):593–604. doi:10.1016/j.renene.2003.07.002
Cripps E, Nott D, Dunsmuir WTM, Wikle C (2005) Space-time modelling of Sydney Harbour winds. Aust N Z J Stat 47(1):3–17. doi:10.1111/j.1467-842X.2005.00368.x
Daniel AR, Chen AA (1991) Stochastic simulation and forecasting of hourly average wind speed sequences in Jamaica. Solar Energy 46(1):1–11
Dorfleitner G, Wimmer M (2010) The pricing of temperature futures at the Chicago Mercantile Exchange. J Bank Finance. doi:10.1016/j.bankfin.2009.12.004
Dorvlo ASS (2002) Estimating wind speed distribution. Energy Convers Manage 43 (17):2311–2318. doi:10.1016/s0196-8904(01)00182-0
Garcia A, Torres JL, Prieto E, de Francisco A (1998) Fitting wind speed distributions: a case study. Solar Energy 62(2):139–144. doi:10.1016/s0038-092x(97)00116-3
Haslett J, Raftery AE (1989) Space-time modelling with long-memory dependence: assessing Ireland's wind power resource. J R Stat Soc Ser C (Appl Stat) 38(1):1–50
Huang Z, Chalabi ZS (1995) Use of time-series analysis to model and forecast wind speed. J Wind Eng Ind Aerodyn 56:311–322
Huang H-H, Shiu Y-M, Lin P-S (2008) HDD and CDD option pricing with market price of weather risk for Taiwan. J Futures Mark 28(8):790–814
Jaramillo OA, Borja MA (2004) Wind speed analysis in La Ventosa, Mexico: a bimodal probability distribution case. Renew Energy 29(10):1613–1630. doi:10.1016/j.renene.2004.02.001
Jewson S, Brix A, Ziehmann C (2005) Weather derivative valuation: the meteorological, statistical, financial and mathematical foundations. Cambridge University Press, Cambridge, UK
Justus CG, Hargraves WR, Mikhail A, Graber D (1978) Methods for estimating wind speed frequency distributions. J Appl Meteorol (United States) 17(3):350–385
Kamal L, Jafri YZ (1997) Time-series models to simulate and forecast hourly averaged wind speed in Quetta, Pakistan. Solar Energy 61(1):23–32
Kavak Akpinar E, Akpinar S (2005) A statistical analysis of wind speed data used in installation of wind energy conversion systems. Energy Convers Manage 46(4):515–532. doi:10.1016/j.enconman.2004.05.002
Kavasseri RG, Seetharaman K (2009) Day-ahead wind speed forecasting using f-ARIMA models. Renew Energy 34(5):1388–1393. doi:10.1016/j.renene.2008.09.006
Lei M, Shiyan L, Chuanwen J, Hongling L, Yan Z (2009) A review on the forecasting of wind speed and generated power. Renew Sustain Energy Rev 13(4):915–920. doi:10.1016/j.rser.2008.02.002
Martin M, Cremades LV, Santabarbara JM (1999) Analysis and modelling of time-series of surface wind speed and direction. Int J Climatol 19:197–209
Mohandes MA, Rehman S, Halawani TO (1998) A neural networks approach for wind speed prediction. Renew Energy 13(3):345–354. doi:10.1016/s0960-1481(98)00001-9
Mohandes MA, Halawani TO, Rehman S, Hussain AA (2004) Support vector machines for wind speed prediction. Renew Energy 29(6):939–947. doi:10.1016/j.renene.2003.11.009
Moody JE, Utans J (1992) Principled architecture selection for neural networks: applications to corporate bond rating prediction. In: Refenes AP (ed) Neural networks in the capital markets. Wiley, Chichester/New York
More A, Deo MC (2003) Forecasting wind with neural networks. Marine Struct 16:35–49
Nfaoui H, Buret J, Sayigh AAM (1996) Stochastic simulation of hourly average wind speed sequences in Tangiers (Morocco). Solar Energy 56(3):301–314. doi:10.1016/0038-092x(95)00103-x
Nielsen TS, Madsen H, Nielsen HA, Pinson P, Kariniotakis G, Siebert N, Marti I, Lange M, Focken U, Bremen LV, Louka G, Kallos G, Galanis G (2006) Short-term wind power

forecasting using advanced statistical methods. Paper presented at the European wind energy conference, EWEC, Athens
Pinson P, Kariniotakis GN (2003) Wind power forecasting using fuzzy neural networks enhanced with on-line prediction risk assessment. In: Power Tech conference proceedings, 2003 IEEE, vol 2, Bologna, 23–26 June 2003, p 8
Rehman S, Halawani TO (1994) Statistical characteristics of wind in Saudi Arabia. Renew Energy 4(8):949–956. doi:10.1016/0960-1481(94)90229-1
Saltyte-Benth J, Benth FE (2010) Analysis and modelling of wind speed in New York. J Appl Stat 37(6):893–909
Sfetsos A (2000) A comparison of various forecasting techniques applied to mean hourly wind speed time-series. Renew Energy 21:23–35
Sfetsos A (2002) A novel approach for the forecasting of mean hourly wind speed time series. Renew Energy 27:163–174
Tol RSJ (1997) Autoregressive conditional heteroscedasticity in daily wind speed measurements. Theor Appl Climatol 56:113–122
Tolman HL, Booij N (1998) Modeling wind waves using wavenumber-direction spectra and a variable wavenumber grid. Global Atmos Ocean Syst 6:295–309
Torres JL, Garcia A, De Blas M, De Francisco A (2005) Forecast of hourly average wind speed with ARMA models in Navarre (Spain). Solar Energy 79:65–77
Tuller SE, Brett AC (1984) The characteristics of wind velocity that favor the fitting of a Weibull distribution in wind speed analysis. J Clim Appl Meteorol 23(1):124–134
Wilks DS (2011) Statistical methods in the atmospheric sciences, vol 100, 3rd edn, International geophysics series. Academic, Oxford, UK
WRMA (2009) Celebrating 10 years of weather risk industry growth. http://www.wrma.org/pdf/WRMA_Booklet_%20FINAL.pdf. Accessed Aug 2009
WRMA (2010) Weather derivatives volume plummets. www.wrma.org/pdf/weatherderivatives-volumeplummets.pdf. Accessed Jan 2010
Yamada Y (2008) Simultaneous optimization for wind derivatives based on prediction errors. In: American control conference, Washington, DC, 11–13 June 2008. pp 350–355
Zapranis A, Alexandridis A (2008) Modelling temperature time dependent speed of mean reversion in the context of weather derivative pricing. Appl Math Finance 15(4):355–386
Zapranis A, Alexandridis A (2009) Weather derivatives pricing: modelling the seasonal residuals variance of an Ornstein-Uhlenbeck temperature process with neural networks. Neurocomputing 73:37–48
Zapranis A, Alexandridis A (2011) Modeling and forecasting cumulative average temperature and heating degree day indices for weather derivative pricing. Neural Comput Appl 20(6):787–801. doi:10.1007/s00521-010-0494-1
Zapranis A, Refenes AP (1999) Principles of neural model identification, selection and adequacy: with applications to financial econometrics. Springer, London/New York